Particle rapidity distributions in Pb+Pb and Au+Au high-energy collisions from the Ultra-relativistic Quantum Molecular Dynamics (UrQMD 3.3p2) model at E_{elb} = 200 AGeV.

T.E Nemakhavhani

Physics Department, University of Johannesburg, P.O.Box 524. Auckland Park 2006, Johannesburg, RSA.

E-mail: tnemakhavhani@uj.ac.za

Abstract. The Ultra-relativistic Quantum Molecular Dynamic model (UrQMD 3.3p2) is a microscopic model based on a phase space description of nuclear reaction and it can now support the Large Hadron Collider energies (LHC) of up to a $\sqrt{s_{nn}}$= 14 TeV. This model is used to simulate the ultra-relativistic heavy-ion collisions of finite matter between Pb+Pb and Au+Au collisions at an energy of E_{elb} = 200 AGeV and t = 400-2 fm/c. The simulated results are then used to calculate the rapidity distributions and particle ratios of both mesons particles (π, ρ, η, and K) and baryons particles (p and $\bar{p}$). The rapidity results show that at early time t the rapidity of all three light mesons is maximum at mid-rapidity and that of (p and $\bar{p}$) are depicted at mid-rapidity for both Pb+Pb and Au+Au collisions. The time evolution of rapidity distributions for Au+Au and Pb+Pb collisions reaches saturation time at different time intervals. The particle ratios between different particle species are then compared between that of Pb+Pb collisions with that of Au+Au collisions. The results are in good agreement with both systems and with the previous studies done.

1. Introduction

A large number of studies in heavy ion physics and high energy physics have been done using the results from the Relativistic Heavy Ion Collider (RHIC) but now with the restart of the Large Hadron Collider (LHC) physics programme, the field of high energy nuclear physics, and especially heavy ion physics, has gone into a new era [1, 2]. It is now possible to explore the properties of Quantum-Chromo-Dynamics (QCD) at unprecedented particle densities and temperatures, and at much higher energies than that produced at RHIC, from $\sqrt{s}$ = 200 GeV to $\sqrt{s}$ = 14 TeV at the LHC [3]. High energy heavy ion reactions are studied experimentally and theoretically to obtain information about the properties of nuclear matter under extreme conditions at high densities and temperatures, the phase transition of a new state of matter and the quark-gluon plasma (QGP) [4, 5].

This work reports on particle rapidity distributions in Pb+Pb and Au+Au high-energy collisions from the Ultra-relativistic Quantum Molecular Dynamics (UrQMD 3.3p2) model at E_{elb} = 200 AGeV. The study will focus on the comparison of the two systems of Pb+Pb and Au+Au collisions and determines if they are the same or different by studying the rapidity distributions of hadronic particles at different time steps. The study of the distribution as a function of time will also give insights into whether the two systems do reach a phase transition at

the same time, which has been poorly documented as many studies focus on energy distributions and comparing data simulated from models with experimental data, instead of the time evolution of heavy-ion collisions [6, 7]. The particle ratios will help us to understand the particle production between the two systems, which will help in the understanding of the effect of different degrees of freedom and phase transitions that lead to the final state of particle production [8]. The study will help in the continuous development and updating of the models such as the UrQMD model and as well as the future development of the high energy heavy ion experiments such as LHC and RHIC.

The rest of the paper is organized as follows: In section 2 we study the description of the UrQMD model. In section 3 we study the particle rapidity distributions in Pb+Pb and Au+Au high-energy collisions, concluding in section 4.

2. Brief description of the UrQMD model

The UrQMD is a microscopic model based on a phase space description of nuclear reactions. We use version 3.3p2 of the UrQMD model for this study as the latest version of UrQMD-3.4 is currently unstable while compiling [9, 10, 11]. The UrQMD 3.3p2 hybrid approach extends previous ansatzes to combine the hydrodynamic and the transport models for relativistic energies.The UrQMD model describes the phenomenology of hadronic interactions at low and intermediate energies from a few hundred MeV up to the new LHC energy of $\sqrt{s}$ =14 TeV per nucleon in the center of mass system [12, 13]. The UrQMD collision term contains 55 different baryon species and 32 meson species, which are supplemented by their corresponding anti-particles and all the isospin-projected states [10, 12, 14]. The properties of the baryons and the baryon-resonances which can be populated in UrQMD can be found in [10, 14], together with their respective meson and the meson resonances. A collision between two hadrons will occur if

$$d_{trans} \leq \sqrt{\frac{\sigma_{tot}}{\pi}}, \qquad \sigma_{tot} = \sigma(\sqrt{s}, type), \tag{1}$$

where d_{trans} and σ_{tot} are the impact parameter and the total cross-section of the two hadrons respectively [12, 14]. In the UrQMD model, the total cross-section σ_{tot} depends on the isospins of colliding particles, their flavour and the centre-of-mass (c.m) energy $\sqrt{s}$. More details about the UrQMD model are presented in Refs. [12, 13, 14].

3. Particle rapidity distributions

This section focuses on the different results of the particle rapidity distributions in Pb+Pb and Au+Au high-energy collisions. The results will be discussed as follows: in subsection 3.1 we look at the rapidity distributions results for meson particles, namely the pions π, the rhos ρ, the etas η, and the kaons K. In subsection 3.2: similar analysis is done as in subsections 3.1 but this time the focus is on baryon species, namely the proton(p) and the anti-proton($\bar{\text{p}}$). The study then compares the particle rapidity distributions at a lower time of t = 2 fm/c with that of a later time after the heavy-ion collisions at t = 198 fm/c. In subsection 3.4 we then look at the time evolution of particle rapidity distributions in Au+Au and Pb+pb high-energy collisions for both mesons and baryon species and find the saturation times leading to phase transitions. Lastly, in subsection 3.5 the study compares the particle ratios for both Pb+Pb and Au+Au high-energy collisions.

3.1. Rapidity distributions of mesons: π, ρ, η and K

Here we observe that in both figure 1 at t = 2 fm/c and figure 2 at t = 198 fm/c both the two systems of Au+Au and Pb+Pb high-energy collisions are comparable with each other. In both systems, at t = 2 fm/c we also observes that less particles are produced at mid-rapidity just below $dN/dy \simeq 80$ for pions and just below $dN/dy \simeq 20$ for rhos, etas and kaons when compared

to a later time of t = 198 fm/c and where a large number of particles are now produced above $dN/dy \simeq 200$ for pions and $dN/dy \simeq 48$ for kaons. At higher time t = 198 fm/c it is observed that rhos and etas decay almost completely to form other particles. This is the reason a large number of pions and kaons are observed.

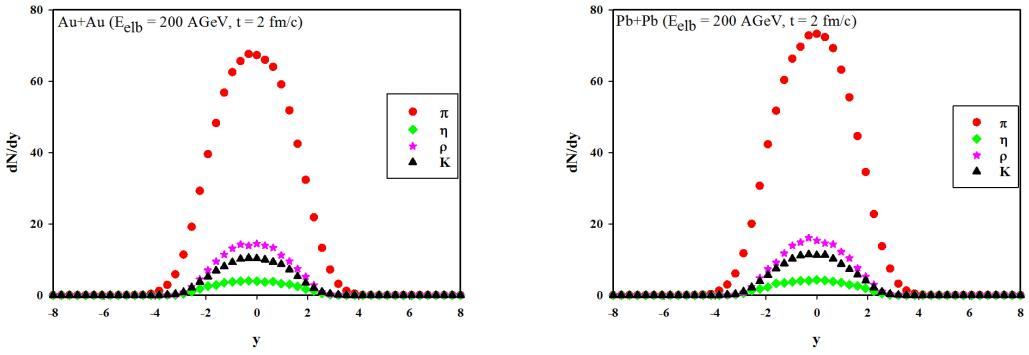

(a) (b)

Figure 1: Particle rapidity distributions in Pb+Pb and Au+Au high-energy collisions for four different meson species: pion(π), rho(ρ), eta(η) and kaon(K) at t = 2 fm/c.

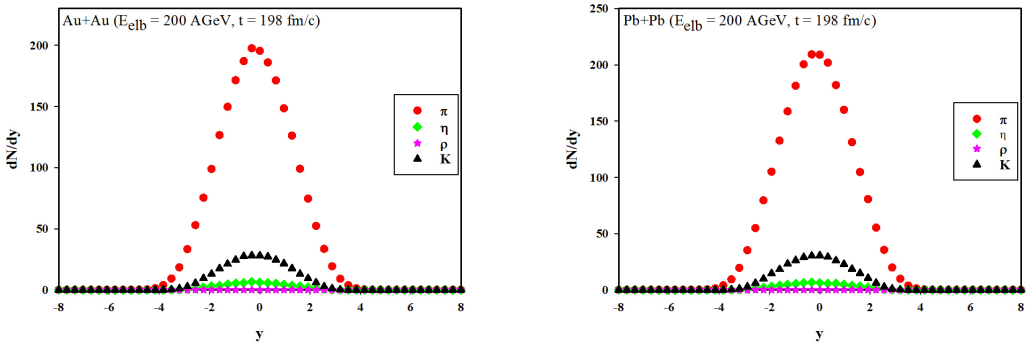

(a) (b)

Figure 2: Particle rapidity distributions in Pb+Pb and Au+Au high-energy collisions for four different meson species: pion(π), rho(ρ), eta(η) and kaon(K) at t = 198 fm/c.

3.2. Rapidity distributions of baryons: p and $\bar{p}$

In this subsection it is observed that in both figure 3 at t = 2 fm/c and figure 4 at t = 198 fm/c both systems Au+Au and Pb+Pb, are comparable with each other. At t = 2 fm/c we observe that less particles are produced at mid-rapidity, around $dN/dy \simeq 5$ for both p and $\bar{p}$ in both systems when compared to that of a later time of t = 198 fm/c, where a large number of particles were produced just above $dN/dy \simeq 14$ for both p and $\bar{p}$ respectively. In figure 3 it is observed that particle rapidity distributions are depicted at mid-rapidity, and this is due to the mid-rapidity at an early time in the system still being very hot and dominated by mesons. Similarly, at the later time of t = 198 fm/c in figure 4 at mid-rapidity, the rapidity distribution for both baryon species behaves like a Gaussian curve. The reason behind this behaviour is because at a

later time (after the collision) the systems have now cooled down and are dominated by baryon species. The inserts in both figures show the actual behaviour of rapidity distributions in both systems.

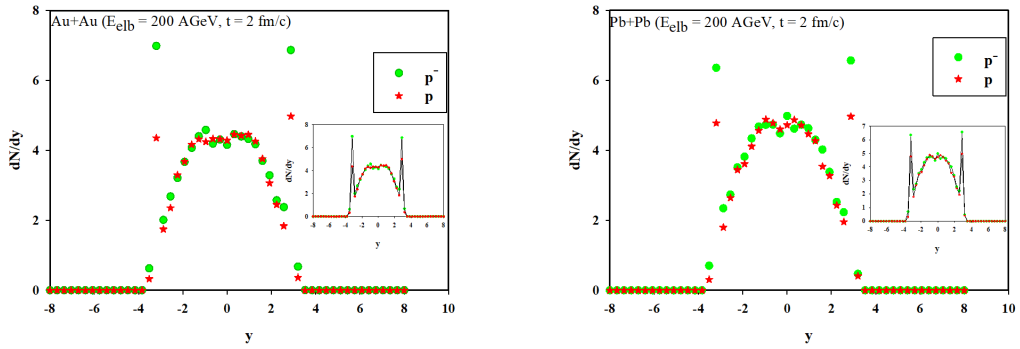

(a) **(b)**

Figure 3: Particle rapidity distributions in Pb+Pb and Au+Au high-energy collisions for baryon particles proton(p) and anti-proton($\bar{p}$) at t = 2 fm/c.

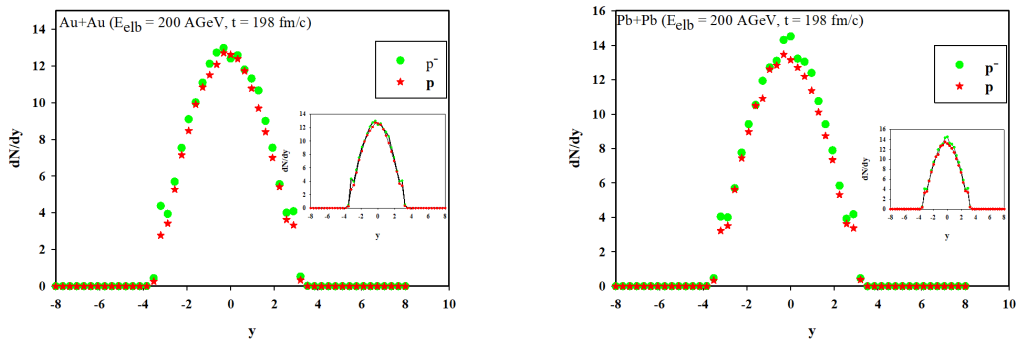

(a) **(b)**

Figure 4: Particle rapidity distributions in Pb+Pb and Au+Au high-energy collisions for baryon particles proton(p) and anti-proton($\bar{p}$) at t = 198 fm/c.

3.3. Time evolution of rapidity distributions for mesons: π, ρ, η and K

In this subsection, we now focus on the time evolution of rapidity distribution in Au+Au and Pb+Pb high-energy collisions for meson species. In figure 5 (a) and (b) we observe that particle rapidity distributions saturates with time for both systems. The saturation for (a) is around t $\simeq$ 50 fm/c and for (b) it is around t $\simeq$ 60 fm/c. The difference in saturation time is that (a) is a smaller system and (b) is a larger system.

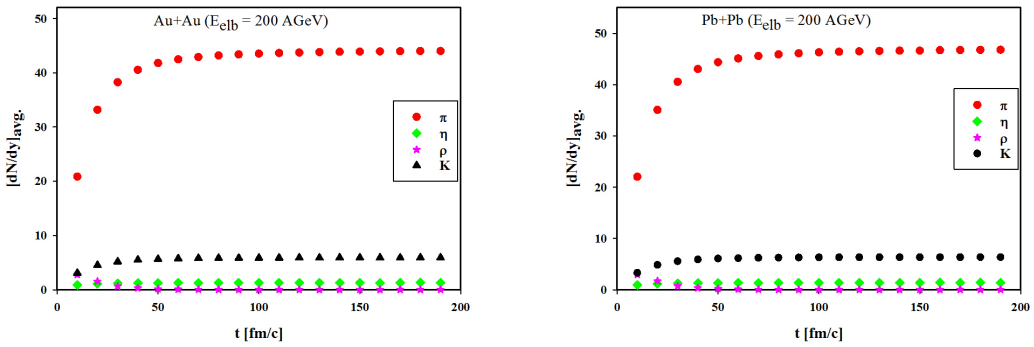

(a) (b)

Figure 5: Time evolution of particle rapidity distributions in Pb+Pb and Au+Au high-energy collisions for four different mesons species pion(π), rho(ρ), eta(η) and kaon(K).

3.4. Time evolution of rapidity distributions for baryons particles: p and $\bar{p}$

As in subsection 3.3 we now focus on the baryon species. The same behaviour as in subsection 3.3 is observed but now the saturation time of the baryon species in both systems is higher. In figure 6 (a) and (b) it is observed that the particle rapidity distribution saturation for (a) is around t $\simeq$ 70 fm/c and for (b) is around t $\simeq$ 80 fm/c. The saturation times for both systems are higher than that of meson species because baryons are only formed and dominate the systems at a later time after the high-energy collisions.

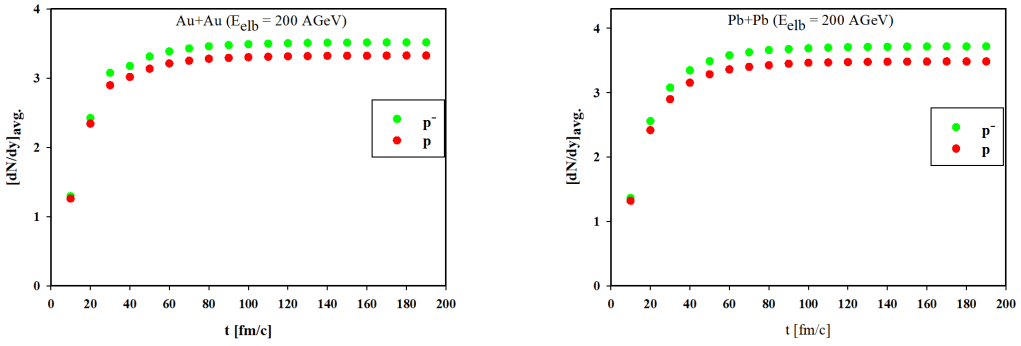

(a) (b)

Figure 6: Time evolution of particle rapidity distributions in Pb+Pb and Au+Au high-energy collisions for baryon particles: proton(p) and anti-proton($\bar{p}$).

3.5. Au+Au and Pb+Pb particle ratios.

This subsection discusses the particle ratios of both Pb+Pb and Au+Au high-energy collisions at different time intervals t = 2 fm/c and t = 198 fm/c. In both table 1 and 2 different behaviour of particle ratios between mesons to mesons and baryons to mesons with time are observed. In both tables p/π^+ and K^+/π^+ increase with time, and $\bar{p}/\pi^-$ and K^-/π^- decrease with time. The results between the two systems are very much comparable regardless of the other system being heavier than the other.

Table 1: Au+Au high-energy collisions particle ratios.

time fm/c	p/π^+	$\bar{p}/\pi^-$	K^-/π^-	K^+/π^+
2	0.19	0.28	0.21	0.14
198	0.24	0.24	0.20	0.21

Table 2: Pb+Pb high-energy collisions particle ratios.

time fm/c	p/π^+	$\bar{p}/\pi^-$	K^-/π^-	K^+/π^+
2	0.19	0.27	0.22	0.14
198	0.23	0.24	0.20	0.21

4. Conclusion

From the presented results, it is observed that particle rapidity distributions for both mesons and baryons are comparable to both larger systems (Pb+Pb) and smaller systems (Au+Au) collisions at t = 2 fm/c and t = 198 fm/c. At mid-rapidity, it is observed that the distributions increase with time for pions and kaons while decreasing with time for rhos and etas. This is due to these particles decaying to form extra pions and kaons. Similarly for baryons, at mid-rapidity at t = 2 fm/c, a depiction of both protons and anti-protons is observed such that at the higher time t = 198 fm/c they both behave like mesons, and this is because baryons only dominate the system at mid-rapidity at a very later time after the heavy ion collisions when both systems have cooled down. The time evolution of the rapidity distributions shows that both systems reach phase transitions at different times for mesons and baryons and lastly, the particle ratios for both systems are comparable with each other. As such, one can conclude that both systems are very much comparable with each other at lower and higher times at E_{elb} = 200 AGeV. Both systems reach phase transitions at different times, which will help in understanding the different stages of nuclear collisions, phase transitions, and chemical freeze out formed at different times after collisions. The results are again comparable to the previous studies done, even though with different systems, energies, models, and experimental data [7, 8, 15].

5. Acknowlegments

I would like to thank everyone who helped me with this paper in terms of corrections and discussions. Financial support from UJ Department of Physics is acknowledged.

References

[1] Reichert T and Bleicher M 2022 *arXiv preprint arXiv:2206.00410*
[2] Xu J, Yu S, Liu F, Luo X *et al.* 2016 *Physical Review C* **94** 024901
[3] Campbell J M, Ellis R K and Williams C 2011 *Journal of High Energy Physics* **2011** 1–36
[4] Demir N and Wiranata A 2014 *Journal of Physics: Conference Series* vol 535 (IOP Publishing) p 012018
[5] Chen Z, Greiner C, Xu Z and Zhuang P 2019 *Physical Review C* **100** 014906
[6] Gao L N, Liu F H, Sun Y, Sun Z and Lacey R A 2017 *The European Physical Journal A* **53** 1–11
[7] Li Q, Wang Y, Wang X and Shen C 2016 *SCIENCE CHINA Physics, Mechanics & Astronomy* **59** 1–4
[8] Kundu S K, Bailung Y, Rode S P, Bhaduri P P and Roy A 2021 *Physical Review C* **104** 024907
[9] Hussain N and Bhattacharjee B 2017 *Physical Review C* **96** 024903
[10] Collaboration U *et al.* The urqmd user guide (2014)
[11] Vovchenko V Y, Anchishkin D and Gorenstein M 2015 *Nuclear Physics A* **936** 1–5
[12] Bleicher M, Zabrodin E, Spieles C, Bass S A, Ernst C, Soff S, Bravina L, Belkacem M, Weber H, Stöcker H *et al.* 1999 *Journal of Physics G: Nuclear and Particle Physics* **25** 1859
[13] collaboration P *et al.* 2005 *Technical Progress Report, GSI, Darmstadt*
[14] Bass S A, Belkacem M, Bleicher M, Brandstetter M, Bravina L, Ernst C, Gerland L, Hofmann M, Hofmann S, Konopka J *et al.* 1998 *Progress in Particle and Nuclear Physics* **41** 255–369
[15] Hoelck J and Wolschin G 2020 *Physical Review Research* **2** 033409